

## Case study

# Predicting the splitting tensile strength of concrete incorporating anacardium occidentale nut shell ash using reactivity index concepts and mix design proportions



Solomon Oyebisi<sup>a,\*</sup>, Tobit Igba<sup>b</sup>, Akeem Raheem<sup>c</sup>, Festus Olutoge<sup>d</sup>

<sup>a</sup> Department of Civil Engineering, Covenant University, PMB 1023, Km 10, Idiroko Road, Ota, Nigeria

<sup>b</sup> Department of Civil Engineering, Federal University of Agriculture, Abeokuta, Nigeria

<sup>c</sup> Department of Civil Engineering, Ladoko Akintola University of Technology, PMB 4000, Ogbomoso, Nigeria

<sup>d</sup> Department of Civil and Environmental Engineering, University of the West Indies, St Augustine, Trinidad and Tobago

## ARTICLE INFO

## Article history:

Received 14 April 2020

Received in revised form 5 June 2020

Accepted 8 June 2020

## Keywords:

Cashew nutshell ash

Supplementary cementitious material

Reactivity indexes

Concrete

Slump

Splitting tensile strength

Compressive strength

Regression model

## ABSTRACT

The prevalence of global warming and climate change are associated with carbon dioxide (CO<sub>2</sub>) emitting from fossil fuel combustion and Portland cement (PC) production. However, in a bid to minimize over-reliance on PC, this study recycled a supplementary cementitious material (SCM), anacardium occidentale nutshell ash (AONSA), for the production of green concrete. AONSA was used as a replacement for Portland limestone cement (PLC) at 0, 5, 10, 15, and 20% using the mix design proportions (MDPs) of grades 25 (M 25), 30 (M 30), and 40 (M 40) concrete. The chemical compositions of both AONSA and PLC were analyzed. Moreover, the chemical moduli of each and mixed binder were determined and evaluated, hence quantifying the reactivity indexes (RIs). Consequently, RIs and MDPs were applied to predict the splitting tensile strength. Compared with the experimental results, the predictive splitting tensile strength relative to the RIs and the MDPs yielded a high precision with 95% R<sup>2</sup> at 28 days curing. Therefore, the model equations proposed by this study can be applied to the concrete mix design procedure for the splitting tensile strength of green concrete incorporating SCMs provided the chemical compositions of each and mixed material are established.

© 2020 The Author(s). Published by Elsevier Ltd. This is an open access article under the CC BY license (<http://creativecommons.org/licenses/by/4.0/>).

## 1. Introduction

The global contribution of Portland cement (PC) production to greenhouse gas emissions (GHG) is estimated to be about 1.35 billion tonnes annually or about 7% of the total GHG to the earth's atmosphere [1]. The primary sources of GHG are the emissions from cement production, fossil fuel combustion and other industrial processes [1]. Fan and Miller [2] established that cement production, fossil fuel combustion and other industrial processes account for almost 68% of total global GHG, and were estimated to be 37.90 Gt carbon dioxide (GtCO<sub>2</sub>) in 2018 with Nigeria emitting 0.026 GtCO<sub>2</sub> in 1970 and 0.89 GtCO<sub>2</sub> in 2018. The manufacture of PC has a remarkable influence on the GHG, and consequently, environmental impacts [1]. Moreover, a tonne's production of PC emits 1.1 tonnes of carbon dioxide into the environment [3]. These impacts are contrary to the list of sustainable development goals for good health and wellbeing [4]. The most potential solution to the growing challenges of GHG is by utilizing more considerable amounts of supplementary cementitious materials (SCMs) as a full or

\* Corresponding author.

E-mail address: [solomon.oyebisi@covenantuniversity.edu.ng](mailto:solomon.oyebisi@covenantuniversity.edu.ng) (S. Oyebisi).

partial replacement with PC for sustainable products, infrastructures, and development [5–7]. It was reported that about 67 % energy requirement and 80 % material cost are reduced when up to 50 % pozzolan of PC weight is utilized as SCM [8]. Also, with 25 % addition of pozzolan, both energy requirement and material cost are reduced by about 33 and 20 %, respectively [8].

Cashew (*Anacardium Occidentale*) nutshell is agricultural by-product with an estimated generation of 4,430,341 metric tonnes (MT), 4,087,563 MT, and 3,971,046 MT in 2015, 2016, and 2017, respectively, in the world [9]. In contrast, Nigeria generated 97,149 MT, 98,291 MT, and 98,253 MT in 2015, 2016, and 2017, respectively [9]. Between 2005 and 2014, there was about a 12 % annual increase in cashew production in the West African region [10]. The West African region has become the largest producer of cashew nut in the world, with about 1,350,000 MT, before Asian countries (India, Vietnam, Cambodia, Indonesia), which produces about 1,300,000 MT [9,11]. Cashew nutshell contains about 30–35 wt% oil called cashew nut shell liquid [12]. Also, about 1,825,000 MT waste is generated from 2,500,000 MT production of cashew nuts [13]. However, it is perturbing to observe that these wastes are discarded indiscriminately, hence causing environmental degradation. The huge disposal of cashew nutshell motivates this study to valorize it as a replacement for PC to produce green concrete. Pyrolysis is one of the widely used valorization methods for a large number of cashew nutshells [11,14,15]. During the pyrolysis, cashew nutshells are transformed into the liquid for industrial chemical synthesizers [12], pharmaceutical drugs [16], and energy [11]; ashes for improving the packing factor and creep resistance of asphalt concrete [14]; oil as lubricants to improve viscosity and wear resistance [17], or as biodiesel [18,19], and fuel to replace woods and charcoals [20]. Moreover, during the pyrolysis of cashew nutshells, about 82 wt% of processed hulls is recovered as gas and 18 wt% as ash [13]. Some researchers also utilized cashew nutshell ash as a PC replacement for the production of concrete. Oyebisi et al. [21] investigated the performance of concrete incorporated with *anacardium occidentale* nutshell ash (AONSA). It was revealed that the concrete exhibited higher resistance against sulfate and acidic attacks than PCC. Also, workability properties, slump and compacting factor of the fresh concrete increased with increasing AONSA content in the mix. Similarly, Pandi and Ganesan [22], Pandi et al. [23], and Thirumurugan et al. [24] evaluated the permeability and compressive effects of concrete incorporated with AONSA. It was indicated that the compressive strength increased with increasing AONSA content up to 25 % maximum substitution in the mix.

Other SCMs such as metakaolin (MK), silica fume (SF), rice husk ash (RHA), fly ash (FA), and ground granulated blast furnace slag (GGBFS) have been utilized as a partial or full replacement by PC to improve the concrete properties [25]. The mechanical property of concrete was examined using 5–20 % MK as partial replacement of PC. It was found that up to 15 % of MK improved the mechanical properties of concrete [26]. In another related study, compressive and splitting tensile strengths of concrete incorporated with SF was investigated; the results revealed the highest compressive and splitting tensile strengths at 15 % SF of PC weight [27]. Moreover, the workability, water permeability, and compressive strength of concrete were assessed by replacing PC with RHA; the results indicated a higher compressive strength at 10 % RHA at 90 days curing [28]. Furthermore, the effects of incorporating SCMs on the thermal conductivity and compressive strength of concrete were evaluated [29]. At both 28 and 120 days curing, there was about 19 and 6% increase in compressive strengths at 15 % SF of PC weight compared with 100 % PC. Also, at 120 days curing, there was about a 1% increase in compressive strength at 15 % FA of PC weight compared with 100 % PC [29]. Besides, at both 15 and 30 % GGBFS of PC weight, there was about 14 and 10 % increase in compressive strength, respectively, at 120 days curing compared with 100 % PC [29].

The reactivity indexes (RIs) of mixed binders are obtained following the establishment of oxide compositions [30–32]. Moreover, the reactivity of any SCM depends on its fineness, chemical and mineralogical compositions, mix design proportions (MDPs), and specific surface area [30]. Also, type, mineralogical, and chemical structures of aggregates influence the performance and reactivity of concrete [33–35]. However, the responsiveness of SCM cannot be evaluated using a single oxide. Therefore, reactivity, hydraulic, and lime moduli are majorly applied to quantify the hydraulic or self-cementitious properties. In contrast, both silica and alumina moduli are used to determine pozzolanic properties [21,32,36]. Portland cement exhibits strong hydraulic properties owing to its high content in CaO [31]. In contrast, AONSA shows strong pozzolanic response due to its high content in SiO<sub>2</sub> [21,37]. Xie and Visintin [36] and Oyebisi et al. [21] developed models to predict the compressive strengths of concrete incorporating SCMs based on MDPs and RIs. The models yielded high precision, and besides, RIs could be evaluated using the principal oxides, CaO, SiO<sub>2</sub>, Al<sub>2</sub>O<sub>3</sub>, Fe<sub>2</sub>O<sub>3</sub>, MgO, and SO<sub>3</sub>. These principal oxides guide the self-cementitious and pozzolanic reactions of the binding materials.

This study, thus, aims to fill a gap by assessing the reactivity responses of PLC mixed with AONSA. Besides, the study establishes the chemical compositions of each and mixed binder, hence evaluating the RIs of the blended mix. It carries out experimentation via laboratory work to obtain the splitting tensile strength of the concrete incorporating AONSA and uses the data, RIs, and MDPs to predict the relationship. The recycling of AONSA would lessen the environmental, economic, and societal threats posed by PC production; improve the concrete properties, and reduce the construction cost and solid wastes, hence driving sustainability. The developed models would contribute to the improvement of future studies on concrete incorporating SCMs by providing means of predicting splitting tensile strength under an applied load based on the RIs and MDPs such that time and cost for carrying out the laboratory experiments would be reduced.

## 2. Materials and methods

### 2.1. Materials

Anacardium occidentale nutshell ash (AONSA) was obtained following the pyrolysis of anacardium occidentale nutshells obtained from the Federal University of Agriculture, Abeokuta, Nigeria. The valorization was performed at the pyrolysis unit of the Covenant University, Ota, Nigeria. After the pyrolysis, about 20 wt% of processed hulls was retrieved as AONSA. Dangote 3 × 42.5R Portland limestone cement (PLC) was used as a binder for the concrete production. The pH of AONSA and PLC was obtained following the procedure stated in ASTM C 25 [38] by mixing 10 g of binding material (AONSA, PLC) with 200 mL of deionized water, and stirring the mix for 30 min. The mix's pH was measured using Hannah pH digital metre (Model 211 microprocessor), and the results are presented in Table 1. The specific gravity (SG) of the binding materials was determined following the requirements stated by BS EN 196–3 [39] using a specific gravity bottle and kerosene. The results are presented in Table 1. Furthermore, the fineness was obtained by using the dry sieving method and BS sieve 90 μm, as stipulated by BS EN 196–6 [40]. The results are shown in Table 1 and satisfied the 12 % maximum fineness specification stated by BS EN 196–6 [40], hence suitable for use as binder and SCM in concrete production. Moreover, the specific surface area of both AONSA and PLC was carried out following the procedure stated by BS EN 196–6 [40] using the Blaine method at a standard porosity of 0.500. The results are presented in Table 1. Besides, Laser diffraction, Model Beckman Coulter LS-100 was used to analyze the particle size distribution (PSD) of AONSA and PLC, as shown in Fig. 1, over the range size of 0.5 μm–900 μm. The results are indicated in Table 1. As shown in Table 1, the chemical reaction between lime and pH would be activated by decomposing the Si-O-Si link in AONSA, because the pH value is greater than 13 [41]. The specific gravity and particle size of AONSA, as reported in Table 1, are lower than that of PLC, but the fineness and specific surface area are higher than PLC; this revealed the utmost importance of AONA as SCM such that more volume is obtained when AONSA replaces the PLC [37]. Moreover, AONSA would favourably react with the alkaline environment [42], and effectively exhibit a higher capacity to act with Ca(OH)<sub>2</sub> in the concrete [37].

Aggregates were source locally, used and prepared at saturated surface dry conditions before the mix design. Grading, as shown in Fig. 2, and characterization were carried out on the aggregates following the procedure outlined in BS EN 12,620 [43]. Besides, specific gravity (SG) and water absorption (WA) were determined as described in BS EN 12,620 [41] by weighing a 2 kg of each sample, immersing in clean water at 25 °C for 24 h and drying in an oven for 24 h at 110 °C. The results indicated 2.60 and 2.64 g/cm<sup>3</sup> as SG; and 0.7 and 0.8 % as WA, for both fine aggregate (FA) and coarse aggregate (CA), respectively. Besides, the moisture content (MC) was determined following the procedure stated in BS EN 12,620 [43] by using a clean container covered with a lid. The results indicated 0.3 and 0.2 % as MC for both FA and CA, respectively. Fig. 2 shows the PSD of both FA and CA used; and the aggregates satisfied the limits as specified by BS EN 12,620 [43], hence

**Table 1**  
Physical properties of binding materials used.

Properties	AONSA	PLC
pH	13.35	13.10
Specific gravity (g/cm <sup>3</sup> )	2.98	3.15
Fineness (%)	8.10	7.63
Specific surface area (m <sup>2</sup> /kg)	605	375
Mean particle size (μm)	19.14	24.13

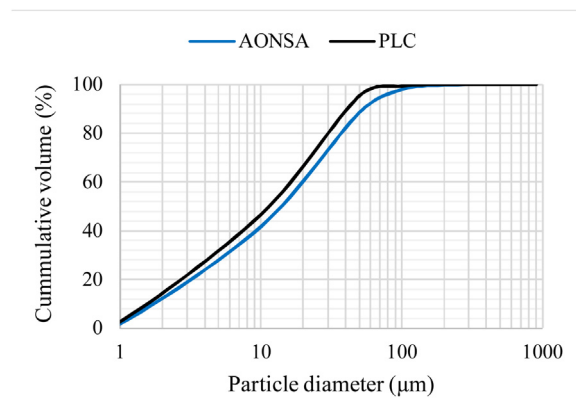


**Fig. 1.** The cumulative particle size distribution of binding materials used. LL is the lower limit; UL is the upper limit

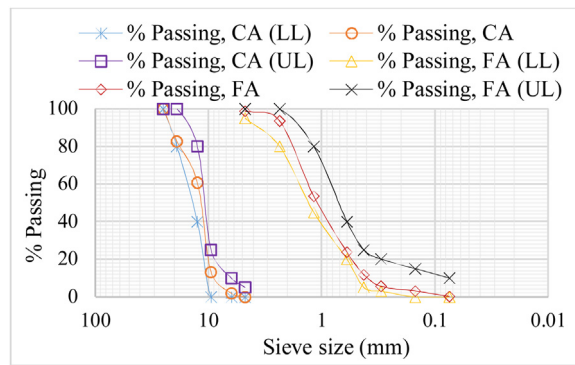


**Fig. 2.** The particle size distribution of aggregates used.

D0 (100 % PLC); D1 (95 % PLC + 5 % AONSA); D2 (90 % PLC + 10 % AONSA); D3 (85 % PLC + 15 % AONSA); D4 (80 % PLC + 20 % AONSA).

suitable for use. On the other hand, the mineralogical composition of the coarse aggregate (granite) was identified with the aid of the Petrological Microscope, Model RPI-3T. The sample was prepared, polished in a glass ground plate using a carborundum, and mounted on a clean glass slide with adhesive [34]. The results revealed quartz, feldspar, mica, and iron oxide of 62.50 %, 20.45, 16.55, and 0.50, respectively. The XRF spectrometer machine, Philips PW-1800 was used to analyze the chemical compositions, and the results indicated SiO<sub>2</sub>, Al<sub>2</sub>O<sub>3</sub>, Fe<sub>2</sub>O<sub>3</sub>, CaO, MgO, SO<sub>3</sub>, K<sub>2</sub>O, Na<sub>2</sub>O, P<sub>2</sub>O<sub>5</sub>, MnO, and LOI as 67.05, 14.40, 5.63, 3.90, 1.72, 0.02, 5.50, 1.16, 0.15, 0.05, and 0.52 %, respectively. From these results, it is inferred that the coarse aggregate is acidic granite because the content of SiO<sub>2</sub> was in the range of 66–75 % [34]. Based on alkalinity, the granite was classified as calcalkalinity in that  $(Na_2O + K_2O)^2 / (SiO_2 - 43)$  was 1.85, hence ranging from 1.2–3.5 for calcalkalinity [35]. Fine aggregate, in its entirety, comprises SiO<sub>2</sub> content [34,44], thus requiring no XRF analysis.

## 2.2. Materials characterization

The chemical compositions of AONSA and PLC were analyzed using the XRF spectrophotometer machine, Philips PW-1800. The results are presented in Table 2. The results indicated that AONSA satisfied the chemical pozzolanic requirements stated in BS EN 450–1 [45] and BS EN 8615–2 [46] such that the addition of SiO<sub>2</sub>, Al<sub>2</sub>O<sub>3</sub>, and Fe<sub>2</sub>O<sub>3</sub> met 70 % minimum requirement. Besides, 5 % maximum of loss of ignition (LOI) recommended by ASTM C 618 [47] and 10 % maximum of LOI recommended by BS EN 450–1 [45] and BS EN 8615–2 [46] for any pozzolanic material were satisfied. The alkali contents, Na<sub>2</sub>O and K<sub>2</sub>O of 5 % maximum, recommended by BS EN 450–1 [45] was also satisfied, hence indicating that the materials would not hinder the concrete performance [48]. Moreover, the addition of SiO<sub>2</sub>, CaO, and MgO  $\geq 67$  % stated by BS EN 3892–1 [49] for a cementitious material was satisfied. It can be deduced that the AONSA could exhibit a pozzolanic reaction and used as the SCM for the production of green concrete, because a SiO<sub>2</sub> content  $\geq 25$  %, stipulated by BS EN 8615–2 [46], and MgO content  $\leq 4$  %, and SO<sub>3</sub> content  $\leq 3$  %, recommended by BS EN 450–1 [45], were met. Moreover, SiO<sub>2</sub> contents of 62.85, 54.85, and 62.85 %, respectively reported by Pandi and Ganesan [22], Pandi et al. [23], Thirmurugan et al. [24], are in line with the SiO<sub>2</sub> content obtained by this study. The chemical compositions of PLC satisfied the oxide specifications stated in BS EN 196–3 [39].

## 2.3. Mix design quantities

The mix quantities were designed following the BS EN 206 [50]'s procedure. The percentage replacement of PLC by AONSA was selected based on the 20–25 % maximum replacement from applicable studies [21–24] to meet the target strengths for structural applications. Thus, PLC was replaced with AONSA at 0, 5, 10, 15, and 20 % for the production of green concrete, denoting as D0, D1, D2, D3, and D4, respectively. The mixes were designed to attain the target strengths 25 MPa, 30 MPa, and 40 MPa for grades M 25, M 30, and M 40 concrete, respectively because of their broader and general uses in the construction sector. Tables 3, 4, 5 show the summary of mix design quantities for M 25, M 30, and M 40, respectively.

**Table 2**

Oxide compositions of the binding materials used.

Oxide Composition	CaO (%)	SiO <sub>2</sub> (%)	Al <sub>2</sub> O <sub>3</sub> (%)	Fe <sub>2</sub> O <sub>3</sub> (%)	MgO (%)	K <sub>2</sub> O (%)	Na <sub>2</sub> O (%)	SO <sub>3</sub> (%)	TiO <sub>2</sub> (%)	P <sub>2</sub> O <sub>5</sub> (%)	LOI (%)
AONSA	2.04	65.02	16.28	10.16	1.53	0.52	0.45	1.32	0.01	0.01	2.95
PLC	64.50	21.55	5.50	3.08	1.52	0.61	–	2.03	–	–	1.20

LOI = Loss of Ignition, determined at 800 °C.

**Table 3**  
Mix design quantity for M 25.

Mix ID	PLC (kg/m <sup>3</sup> )	AONSA (kg/m <sup>3</sup> )	FA (kg/m <sup>3</sup> )	CA (kg/m <sup>3</sup> )
D0	340	0	715	1035
D1	323	17	715	1035
D2	306	34	715	1035
D3	289	51	715	1035
D4	272	68	715	1035

Water-to-binder (w/b) ratio = 0.62.

Binder-to-aggregate (b/agg) ratio = 0.19.

**Table 4**  
Mix design quantity for M 30.

Mix ID	PLC (kg/m <sup>3</sup> )	AONSA (kg/m <sup>3</sup> )	FA (kg/m <sup>3</sup> )	CA (kg/m <sup>3</sup> )
D0	390	0	675	1031
D1	370	20	675	1031
D2	350	40	675	1031
D3	330	60	675	1031
D4	310	80	675	1031

Water-to-binder (w/b) ratio = 0.54.

Binder-to-aggregate (b/agg) ratio = 0.23.

**Table 5**  
Mix design quantity for M 40.

Mix ID	PLC (kg/m <sup>3</sup> )	AONSA (kg/m <sup>3</sup> )	FA (kg/m <sup>3</sup> )	CA (kg/m <sup>3</sup> )
D0	500	0	585	1030
D1	475	25	585	1030
D2	450	50	585	1030
D3	425	75	585	1030
D4	400	100	585	1030

Water-to-binder (w/b) ratio = 0.42.

Binder-to-aggregate (b/agg) ratio = 0.31.

## 2.4. Mix preparation, casting and curing

The mix was prepared following the procedures stated in BS 1881–125 [51] and BS EN 12390–2 [52]. The fresh concrete was poured into a standard cube 150 mm<sup>3</sup> and a standard cylinder 150 mm diameter and 300 mm long in 3 layers, and 25 strokes were applied to each layer using a circular cross-sectional rod of  $\Phi$  16 mm and 600 mm length. The samples were cured under 28 °C and 65 % RH and tested at 7, 14, 28, and 90 days.

## 2.5. Experimental tests and analysis

### 2.5.1. Workability test

The slump test was conducted on the fresh concrete samples following the procedure stated in BS EN 12350–2 [53].

### 2.5.2. Mechanical test

The compressive strength ( $f_c$ ) and splitting tensile strength ( $f_t$ ) were determined with the aid of an INSTRON 5000R UTM following the procedure stated by BS EN 12390–3 [54] and BS EN 12390–6 [55], respectively. For each mix ID, three (3) samples were crushed, and the average of the three values was obtained and used for the analysis.

### 2.5.3. Evaluation of reactivity indexes (RIs)

The principal reactive oxides CaO, SiO<sub>2</sub>, Al<sub>2</sub>O<sub>3</sub>, Fe<sub>2</sub>O<sub>3</sub>, MgO, and SO<sub>3</sub>, were used to evaluate the RIs of the each and mixed binder following the establishment of their oxide compositions, which reflect both hydraulic and pozzolanic reactivity [21,31,32,36]. Eqs. 1–5 illustrate the concept of RIs of mixed materials [21,31,32,36].

$$RM = \frac{CaO + MgO + Al_2O_3}{SiO_2} \quad (1)$$

$$HM = \frac{CaO}{SiO_2 + Al_2O_3 + Fe_2O_3} \quad (2)$$

$$LM = \frac{1.0CaO - 0.7SO_3}{2.8SiO_2 + 1.1Al_2O_3 + 0.7Fe_2O_3} \quad (3)$$

$$SM = \frac{SiO_2}{Al_2O_3 + Fe_2O_3} \quad (4)$$

$$AM = \frac{Al_2O_3}{Fe_2O_3} \quad (5)$$

where RM is reactivity modulus;

HM is the hydraulic modulus;

LM is the lime modulus;

SM is the silica modulus;

AM is the alumina modulus.

#### 2.5.4. Prediction of splitting tensile strength ( $f_t$ ) based on RIs, w/b ratio, and b/agg ratio

Either RM, HM, or LM is used to evaluate the hydraulic properties of binding material, while the pozzolanic activity is quantified by the SM and AM [30–32]. Consequently, a linear relationship exists in the correlation between splitting tensile strength and RIs [36]. First, the regression was modelled based on the combination of RM, SM, and AM; HM, SM, and AM; and LM, SM, and AM using the Minitab 17 statistical software. Second, obtaining the splitting tensile strength of the concrete, integration of the RIs of blended binders was performed by normalizing it with an inverse of 0.62, 0.54, and 0.42 w/b ratios obtained for M 25, M 30, and M 40, respectively. Therefore, splitting tensile strength becomes a direct proportion to RIs, but an inverse proportion to w/b ratio. Predicting the parameters in Minitab 17 statistical software, splitting tensile strength's data was set as a response (dependent variable), while the values of RIs were selected as continuous predictors (independent variables).

The role of binder to aggregate ratio in the concrete properties is significant such that it improves the strength of concrete, apart from RIs and water to binder ratio [34,36]. Moreover, a significant improvement is yielded when the binder to aggregate ratio is normalized and correlated with RIs and water to binder ratio [21,36]. It is noteworthy to state that the weight ratio was used to model the binder to aggregate ratio against the volume ratio to obtain an accurate proportion. For each mix, the proportion was determined using its moisture content and specific gravity to improve the packing capacity of binder-aggregate [34,35]. Following the incorporation of water to binder ratio, the fit regression relationship between splitting tensile strength and binder to aggregate ratio was normalized with 0.19, 0.23 and 0.31 binder to aggregate ratios obtained for M 25, M 30, and M 40, respectively. Finally, the splitting tensile strength was predicted based on the RIs, water to binder ratio, and binder to aggregate ratio using the relationship, as illustrated in Eqs. 6–8 [21,36].

$$f_t = \beta + \left( \frac{\alpha_1 RM + \alpha_2 SM + \alpha_3 AM}{w/b} \right) (b/agg) \quad (6)$$

$$f_t = \beta + \left( \frac{\alpha_1 HM + \alpha_2 SM + \alpha_3 AM}{w/b} \right) (b/agg) \quad (7)$$

$$f_t = \beta + \left( \frac{\alpha_1 LM + \alpha_2 SM + \alpha_3 AM}{w/b} \right) (b/agg) \quad (8)$$

where  $\beta$ ,  $\alpha_1$ ,  $\alpha_2$ ,  $\alpha_3$  are the magnitudes of coefficients.

### 3. Results and discussion

#### 3.1. Workability

Fig. 3 presents the slump values for M 25, M 30, and M 40, respectively. It was revealed that the slump reduced with increasing AONSA content in the mix for all concrete grades. There was about 13–40 %, 10–43 %, and 8–47 % decrease in a slump as the AONSA content increased from 5 to 20%. The reason for the decline in slump could be attributed to the finer particle, smaller particle size and specific gravity, and higher specific surface area of AONSA compared with PLC. These

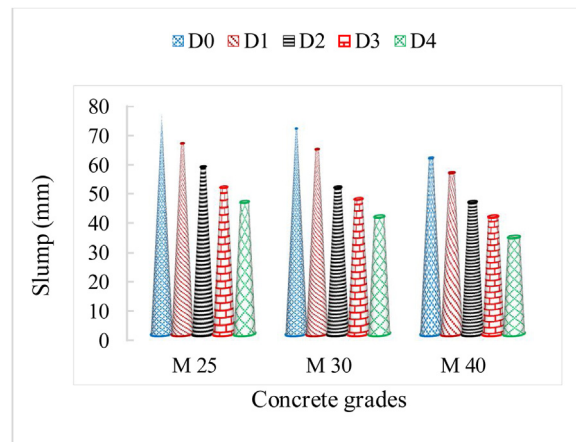


**Fig. 3.** The slump of the fresh concrete.  
D0 (100 % PLC); D1 (95 % PLC + 5 % AONSA); D2 (90 % PLC + 10 % AONSA); D3 (85 % PLC + 15 % AONSA); D4 (80 % PLC + 20 % AONSA).

properties increase the water demands due to more volume and result in highly cohesive and impermeable concrete, hence reducing workability [37]. It was also evident that finer pozzolans (RHA and cashew nut shell ash) reduced the slump of fresh concrete [56,57]. Therefore, a concrete incorporating AONSA could exhibit a cohesive and workable mix up to 20 % replacement because a 150 mm maximum slump recommended by BS EN 12350–2 [53] for standard workable concrete was satisfied.

### 3.2. Mechanical properties

#### 3.2.1. Compressive strength

The results of compressive strengths for M 25, M 30, and M 40 are presented in Fig. 4 (a)–(c), respectively at 7, 14, 28, and 90 days curing. The results indicated that the compressive strengths increased with increasing AONSA content up to 15 % replacement for all concrete grades at all curing ages but at 20 % substitution, the strength reduced marginally. At 28 days curing, there was about 3–6 %, 3–5 %, and 2–5 % increase in compressive strengths as the percentage replacement of PLC by AONSA increased from 5 to 15 % for M 25, M 30, and M 40, respectively compared with the control sample (100 % PLC). The reason for the higher compressive strength due to an increase in AONSA content (15 % maximum) cannot be far-fetched: Anacardium occidentale nutshell ash (AONSA), as shown in Table 2, showed substantial contents of silica oxide ( $\text{SiO}_2$ ) and alumina oxide ( $\text{Al}_2\text{O}_3$ ) compared with PLC. Thus, both silica and alumina oxides reacted with the primary hydrating agents of PLC and resulted in the calcium silicate hydrate (C–S–H) and calcium aluminate hydrate (C–A–H) which are strengthening gel and bonding properties in the concrete, respectively [37]. Moreover, the strength performance of concrete incorporating pozzolan can be associated with the fineness and water demand [58]. Evidence of this was most apparent when the higher strength of fly ash-based concrete was obtained using a finer fraction of fly ash and low water content [59]. This also confirmed that the fineness and low workability of AONSA due to low water content contributed to the higher strength of the concrete. The decrease in strength at 20 % AONSA replacement could be attributed to an excess of AONSA content in the mix; this resulted in low reactivity of silica oxide of AONSA with  $\text{Ca}(\text{OH})_2$  supply and slowed down the formation of hydrating monomers (C–S–H), hence hindering the strength development [56,60]. Notwithstanding, AONSA could be used at 5–20 % replacement level in the production of green concrete because it satisfied the target strengths of concrete grades (classes) specified by BS EN 1992–1–1 [61] at 28 days curing.

#### 3.2.2. Splitting tensile strength

Fig. 5 (a)–(c) present the splitting tensile strengths for M 25, M 30, and M 40, respectively at 7, 14, 28, and 90 days curing. The results revealed that as the AONSA content increased from 5 to 15 %, the splitting tensile strength of the concrete increased. However, the splitting tensile strength slightly decreased at 20 % AONSA substitution, hence indicating 15 % AONSA as the maximum substitution for all concrete grades. At 28 days curing, about 6–15 %, 1–10 %, and 1–9 % increase in splitting tensile strengths were observed as the AONSA content increased from 5 to 15 % for M 25, M 30, and M 40, respectively, compared with the control sample (100 % PLC). It was also evident that the splitting tensile strength of concrete increased with increasing cashew nutshell ash content in the mix [57]. Moreover, at 28–90 days curing, about 2–3 %, 4–7 %, and 12–13 % increase in splitting tensile strengths were noticed as the AONSA content increased from 5 to 15 % for M 25, M 30, and M 40, respectively, compared with about 3, 4, and 6 % for M 25, M 30, and M 40 of control samples, respectively. This indicates that the splitting tensile strength of concrete incorporating AONSA becomes substantial with increasing concrete grades. Therefore, it is inferred that concrete modified with AONSA could resist more tensile strength under an applied load against splitting than that of conventional concrete.

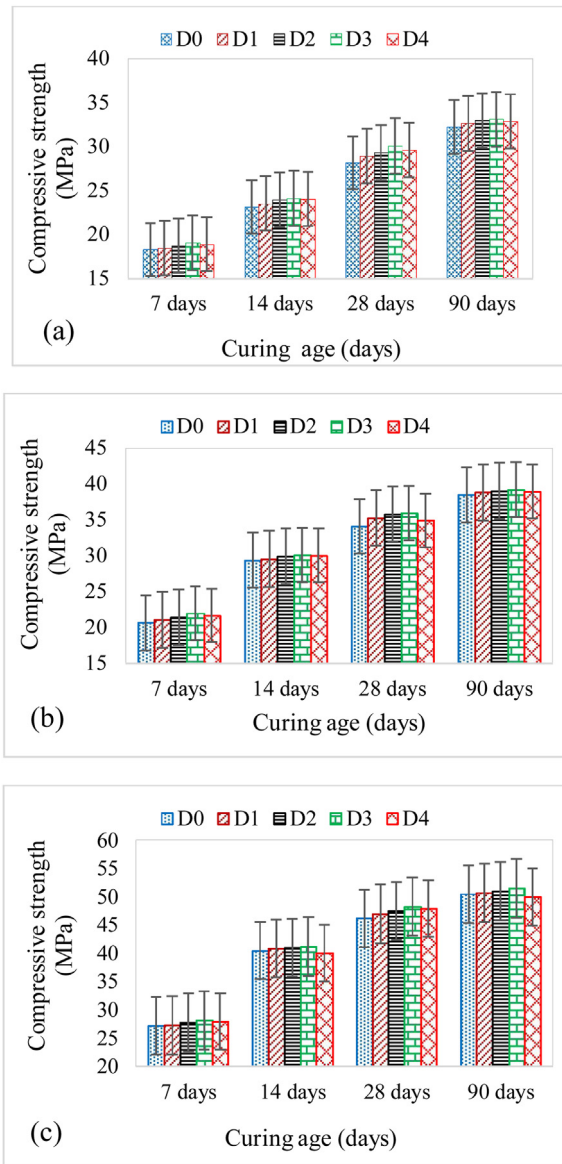


**Fig. 4.** Concrete compressive strengths for (a) grade 25, (b) grade 30, and (c) grade 40. D0 (100 % PLC); D1 (95 % PLC + 5 % AONSA); D2 (90 % PLC + 10 % AONSA); D3 (85 % PLC + 15 % AONSA); D4 (80 % PLC + 20 % AONSA)

### 3.3. Principal reactive oxides of mixed binder

Fig. 6 shows a decrease in CaO and SO<sub>3</sub> contents at 5 % AONSA substitution compared with 100 % PLC composition but gradually increase with increasing AONSA content compared with 5% AONSA replacement. The reason could be attributed to the low contents of CaO and SO<sub>3</sub> in AONSA composition such that both CaO and SO<sub>3</sub> contents were 97 and 35 % respectively lower than that of PLC composition. The blending effect reduced the CaO and SO<sub>3</sub> contents in PLC by 67 and 13 %, 65 and 20 %, and 63 and 19 % at 5 % AONSA replacement for M 25, M 30, and M 40, as shown in Fig. 6 (a)-(c), respectively. However, it was observed that SiO<sub>2</sub>, Fe<sub>2</sub>O<sub>3</sub>, Al<sub>2</sub>O<sub>3</sub>, and MgO contents increased with increasing AONSA content in the mix; this could be associated with the increase in SiO<sub>2</sub>, Fe<sub>2</sub>O<sub>3</sub>, Al<sub>2</sub>O<sub>3</sub>, and MgO contents for AONSA compared with PLC oxide compositions. However, these results were contrary to the related findings reported by Akinwumi and Aidomoje [62] such that the reactive oxides, CaO, MgO, and Al<sub>2</sub>O<sub>3</sub> decrease with the increase in CCA (pozzolan) content; in contrast, SiO<sub>2</sub>, Fe<sub>2</sub>O<sub>3</sub>, and SO<sub>3</sub> increase with increasing CCA content for the CCA-PC blend. Furthermore, Darquennes et al. [30], Sakai et al. [31], and Behim et al. [32] reported that the hydraulicity of a mix increases with increasing CaO, MgO, and Al<sub>2</sub>O<sub>3</sub> contents. However, the pozzolanic increases with increasing SiO<sub>2</sub>, Fe<sub>2</sub>O<sub>3</sub>, and SO<sub>3</sub> contents. This demonstrates that CaO, MgO, and Al<sub>2</sub>O<sub>3</sub> contents contribute to the high phase of amorphous structure in the mix, hence improving the C-S-H formation, and resulting in better strength



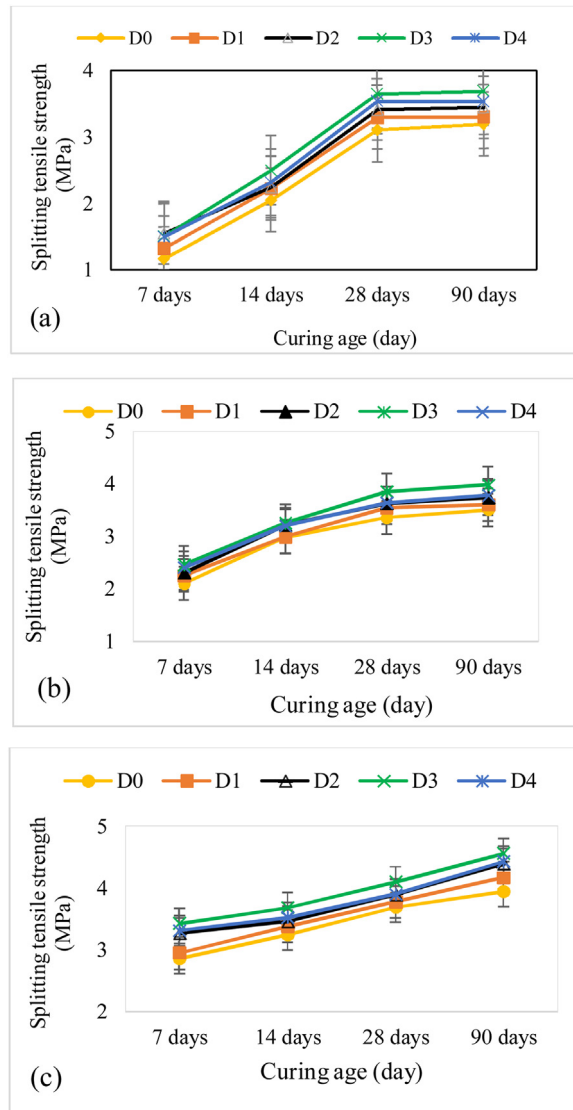


**Fig. 5.** Concrete splitting tensile strengths for (a) grade 25, (b) grade 30, and (c) grade 40. D0 (100 % PLC); D1 (95 % PLC + 5 % AONSA); D2 (90 % PLC + 10 % AONSA); D3 (85 % PLC + 15 % AONSA); D4 (80 % PLC + 20 % AONSA)

performance. Therefore, these assertions could necessitate an increase in splitting tensile strength of concrete with increasing AONSA content up to 15 % maximum compared with PCC (control concrete), as indicated in Fig. 5. Ultimately, it is inferred that the splitting tensile strength of concrete increased with increasing CaO, Al<sub>2</sub>O<sub>3</sub>, MgO, and SiO<sub>2</sub> contents in PLC-AONSA mix at 15 % of AONSA maximum replacement. Therefore, this can benefit the future study by selecting SCMs, which comprise high contents of CaO, Al<sub>2</sub>O<sub>3</sub>, MgO, and SiO<sub>2</sub> to increase the splitting tensile strength in structural concrete.

#### 3.4. RIs of the mixed binder

Following Eqs. 1–5, the RIs of the mixed binder were quantified, and the results are indicated in Fig. 7. Comparing with 100 % PLC, it was revealed that at 5 % AONSA substitution, the RM, HM, LM, SM, and AM decreased, however, they increased with the increase in AONSA content up to 15 % replacement compared with 5 % AONSA substitution, and then, declined slightly at 20 % replacement for all concrete grades. It was also observed that the hydraulic/cementitious responses, RM, HM, and LM of the mixed binders increased with increasing concrete classes (M 25 to M 40). In contrast, the pozzolanic responses, SM and AM decreased with increasing concrete grades (M 25 to M 40). These could be associated with the denser and less porous concrete due to low water content [31,37]. Moreover, it was evident that CaO, Al<sub>2</sub>O<sub>3</sub>, MgO, SiO<sub>2</sub>, Fe<sub>2</sub>O<sub>3</sub>, and SO<sub>3</sub> influenced the RIs of the mixed binder. The RM, HM, and LM of the mixed binder increased with increasing CaO, Al<sub>2</sub>O<sub>3</sub>, MgO contents, while the SM and AM of the mixed binders increased as the content of SiO<sub>2</sub> and Al<sub>2</sub>O<sub>3</sub> increased. Both RM and HM of the mixed

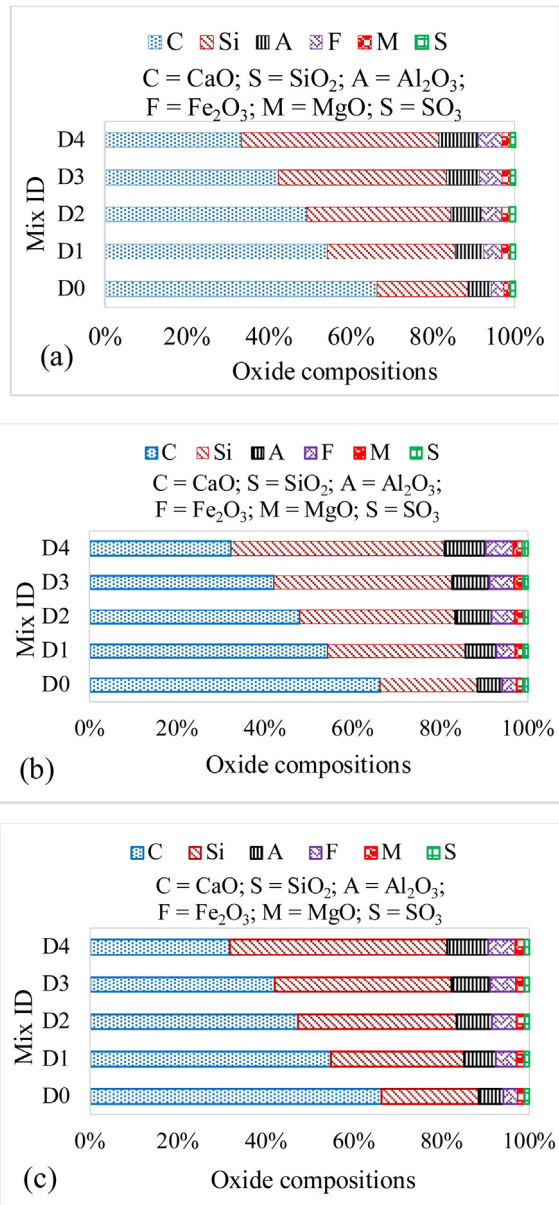


**Fig. 6.** Oxide compositions of the mixed binder for (a) grade 25, (b) grade 30, and (c) grade 40. D0 (100 % PLC); D1 (95 % PLC + 5% AONSA); D2 (90 % PLC + 10 % AONSA); D3 (85 % PLC + 15 % AONSA); D4 (80 % PLC + 20 % AONSA).

binders satisfied the BS EN 8615–2 [46]’s minimum requirement of 1.0. However, the recommended range of  $\geq 0.66 \leq 1.02$  stipulated by BS EN 8615–2 [46] for LM of the mixed binder was not met, except for 100 % PLC; this could be associated with the low ratio of lime to silica, aluminate, and ferrate contents in the PLC-AONSA blend compared with PLC binder.

### 3.5. Prediction of splitting tensile strength ( $f_t$ ) based on RIs, w/b ratio, and b/agg ratio

#### 3.5.1. Prediction of $f_t$ based on RM, AM, SM, w/b ratio, and b/agg ratio

Following the Eq. 6, the results of the statistical data trends are presented in Fig. 8 (a)-(d) for 7, 14, 28, and 90 days, respectively. It was evident that the splitting tensile strength of PLC-AONSA based concrete increased with increasing RM, SM, and AM; this could be associated with the higher contents of CaO, SiO<sub>2</sub>, and Al<sub>2</sub>O<sub>3</sub>, which are predominantly present and active in the PLC and AONSA blend, as shown in Fig. 6, hence increasing the reactive, silica, and alumina responses of the mix. The higher contents of CaO in PLC, and SiO<sub>2</sub> and Al<sub>2</sub>O<sub>3</sub> in AONSA increased the RM, and SM and AM, respectively; and this

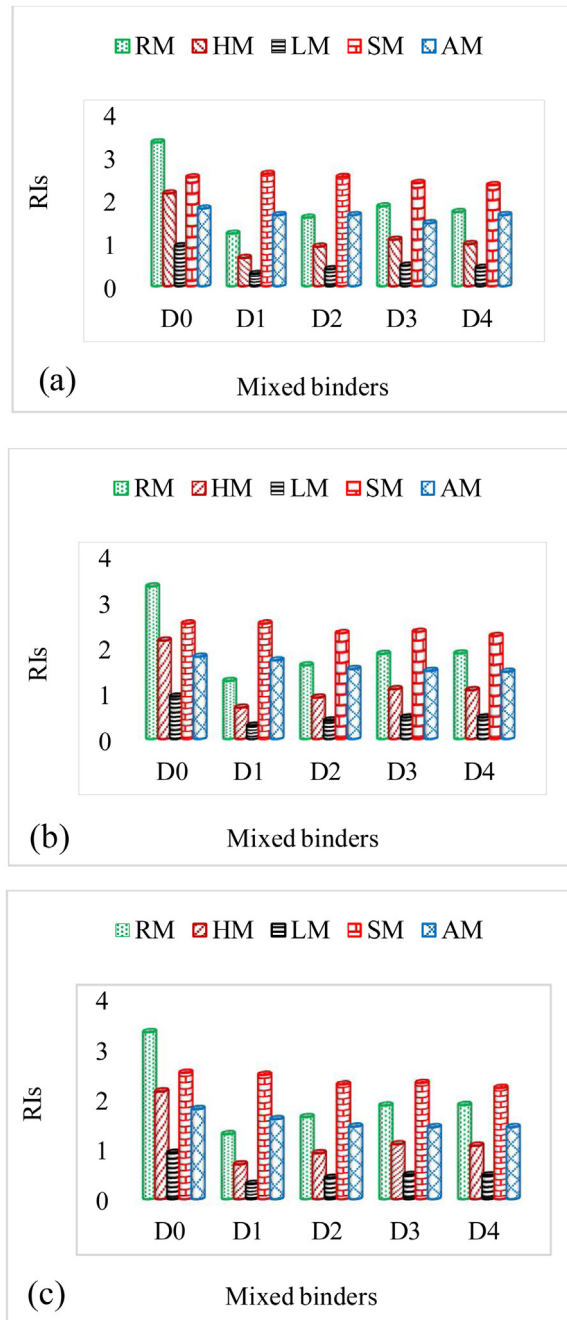


Fig. 7. Reactivity indexes of the mixed binders for (a) grade 25, (b) grade 30, and (c) grade 40.

confirmed the findings reported by Xie and Visintin [36] that the RM, SM, and AM increase with increasing CaO, SiO<sub>2</sub>, and Al<sub>2</sub>O<sub>3</sub> contents. On the other hand, a mix with high contents of CaO, Al<sub>2</sub>O<sub>3</sub>, and MgO exhibits high self-cementitious properties in the presence of water [31]. Ultimately, it is inferred that RM of PLC-AONSA based concrete increases with increasing CaO, SiO<sub>2</sub>, and Al<sub>2</sub>O<sub>3</sub> contents, hence increasing its splitting tensile strength.

The fit regression model was used for the correlation of  $f_t$  based on the RIs (RM, AM, and SM), w/b ratio, and b/agg ratio at the global trend of 95 % confidence interval (CI) and prediction interval (PI). Thus, the regression equations are illustrated in Eqs. 9–12 for 7, 14, 28, and 90 days, respectively. From the regression analysis, the coefficient of determination ( $R^2$ ) was 95, 81, 91, and 98 % fit to predict the data at 95 % CI and PI for 7, 14, 28, and 90 days, respectively. Therefore, these proposed models

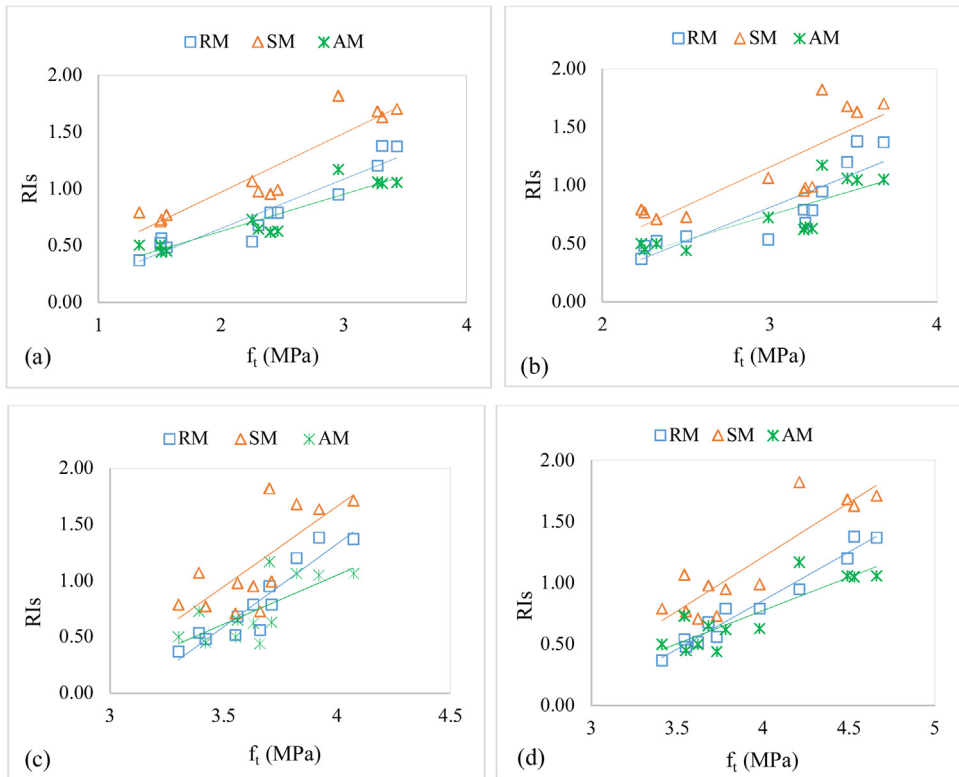


Fig. 8. Statistical data trends between reactivity indexes and splitting tensile strengths at (a) 7, (b) 14, (c) 28, and (d) 90 days.

can be useful in the prediction and development of the splitting tensile strength of concrete incorporating AONSA, particularly in a situation where RM is of great concern.

$$f_{t-7 \text{ days}} = \left\{ \frac{1.402 \text{ RM} - 1.250 \text{ SM} + 3.010 \text{ AM}}{\frac{w}{b}} \right\} \left( \frac{b}{\text{agg}} \right) + 0.441 \quad (9)$$

$$f_{t-14 \text{ days}} = \left\{ \frac{1.165 \text{ RM} - 2.240 \text{ SM} + 3.830 \text{ AM}}{\frac{w}{b}} \right\} \left( \frac{b}{\text{agg}} \right) + 1.808 \quad (10)$$

$$f_{t-7 \text{ days}} = \left\{ \frac{1.402 \text{ RM} - 1.250 \text{ SM} + 3.010 \text{ AM}}{\frac{w}{b}} \right\} \left( \frac{b}{\text{agg}} \right) + 0.441 \quad (11)$$

$$f_{t-14 \text{ days}} = \left\{ \frac{1.165 \text{ RM} - 2.240 \text{ SM} + 3.830 \text{ AM}}{\frac{w}{b}} \right\} \left( \frac{b}{\text{agg}} \right) + 1.808 \quad (12)$$

$$f_{t-28 \text{ days}} = \left\{ \frac{0.784 \text{ RM} + 0.233 \text{ SM} - 0.660 \text{ AM}}{\frac{w}{b}} \right\} \left( \frac{b}{\text{agg}} \right) + 3.234 \quad (13)$$

$$f_{t-90 \text{ days}} = \left\{ \frac{1.023 \text{ RM} + 1.128 \text{ SM} - 1.524 \text{ AM}}{\frac{w}{b}} \right\} \left( \frac{b}{\text{agg}} \right) + 2.935 \quad (14)$$

3.5.2. Prediction of  $f_t$  based on HM, AM, SM, w/b ratio, and b/agg ratio

Fig. 9 (a)-(d) indicate the statistical data trends for HM, AM, SM, w/b ratio, and b/agg ratio at 7, 14, 28, and 90 days, respectively, following the relationship illustrated in Eq. 7. It was observed that the splitting tensile strength of PLC-AONSA mixed concrete increased with increasing RIs, HM, SM, and AM. The reason for a higher splitting tensile strength as a result of an increase in HM, SM, and AM cannot be far-fetched: PLC exhibited higher content of CaO, while AONSA exhibited higher contents of SiO<sub>2</sub> and Al<sub>2</sub>O<sub>3</sub>, hence resulting in a more robust hydraulic response. Therefore, it is inferred that the HM of PLC-AONSA mixed binder increases with increasing CaO, SiO<sub>2</sub>, and Al<sub>2</sub>O<sub>3</sub> contents, and consequently, increases the splitting tensile strength PLC-AONSA based concrete under an applied load.

The regression equations are illustrated in Eqs. 13–16 for 7, 14, 28, and 90 days, respectively following the correlation of  $f_t$  based on the RIs (HM, AM, and SM), w/b ratio, and b/agg ratio at the 95 % CI and PI. From the regression analysis, R<sup>2</sup> was 95, 82, 92, and 98 % fit to predict the data at 95 % CI and PI for 7, 14, 28, and 90 days, respectively. Therefore, these developed models can be used for the splitting tensile strength's prediction and development of concrete incorporating AONSA, provided the RIs and MDPs are established, especially when HM of a mix is of great challenge.

$$f_{t-7 \text{ days}} = \left\{ \frac{2.224 \text{ HM} - 1.385 \text{ SM} + 3.410 \text{ AM}}{\frac{w}{b}} \right\} \left( \frac{b}{agg} \right) + 0.417 \tag{13}$$

$$f_{t-14 \text{ days}} = \left\{ \frac{1.847 \text{ HM} - 2.330 \text{ SM} + 4.140 \text{ AM}}{\frac{w}{b}} \right\} \left( \frac{b}{agg} \right) + 1.789 \tag{14}$$

$$f_{t-28 \text{ days}} = \left\{ \frac{1.275 \text{ HM} + 0.130 \text{ SM} - 0.406 \text{ AM}}{\frac{w}{b}} \right\} \left( \frac{b}{agg} \right) + 3.215 \tag{15}$$

$$f_{t-90 \text{ days}} = \left\{ \frac{1.646 \text{ HM} + 1.011 \text{ SM} - 1.210 \text{ AM}}{\frac{w}{b}} \right\} \left( \frac{b}{agg} \right) + 2.912 \tag{16}$$

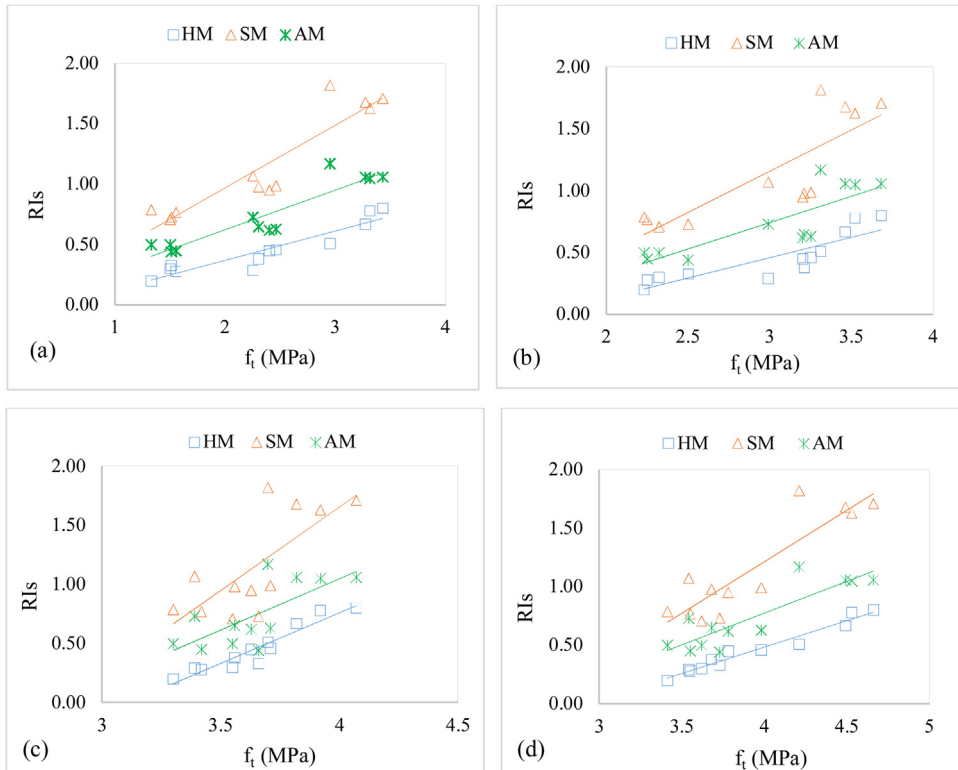


Fig. 9. Statistical data trends between reactivity indexes and splitting tensile strengths at (a) 7, (b) 14, (c) 28, and (d) 90 days.

### 3.5.3. Prediction of $f_t$ based on LM, AM, SM, w/b ratio, and b/agg ratio

Following the Eq. 8, the statistical data trends for LM, AM, SM, w/b ratio, and b/agg ratio are presented in Fig. 10 (a)-(d) for 7, 14, 28, and 90 days, respectively. The splitting tensile strength of PLC-AONSA blended concrete, as shown in Fig. 9, increased with increasing LM, SM, and AM; and this may be attributed to the active and predominant contents of CaO in PLC, and SiO<sub>2</sub> and Al<sub>2</sub>O<sub>3</sub> in AONSA, hence resulting in an increased RIs. Meanwhile, it was noted that LM obtained from this study was out of range of BS EN 8615-2 [46]'s specifications, notwithstanding, a high precision was yielded when it was correlated with SM, AM, and MDPs. Therefore, it is inferred that the LM of PLC-AONSA based concrete increases with increasing CaO, SiO<sub>2</sub>, and Al<sub>2</sub>O<sub>3</sub> contents, hence increasing its splitting tensile strength.

The  $f_t$ , LM, AM, SM, w/b ratio, and b/agg ratio was predicted using the fit regression model at 95 % CI and PI, and the regression equations are illustrated in Eq. 17-20 for 7, 14, 28, and 90 days, respectively. From the regression analysis, R<sup>2</sup> was 94, 81, 90, and 98 % fit to predict the data at the global trend for 7, 14, 28, and 90 days, respectively. Thus, these proposed equations can be applied to the prediction and development of the splitting tensile strength of concrete incorporating AONSA, provided the oxide compositions of the binders, and MDPs are established, most especially when LM is perturbing.

$$f_{t-7 \text{ days}} = \left\{ \frac{4.790 \text{ LM} - 1.325 \text{ SM} + 3.350 \text{ AM}}{\frac{w}{b}} \right\} \left( \frac{b}{\text{agg}} \right) + 0.446 \quad (17)$$

$$f_{t-14 \text{ days}} = \left\{ \frac{3.900 \text{ LM} - 2.250 \text{ SM} + 4.060 \text{ AM}}{\frac{w}{b}} \right\} \left( \frac{b}{\text{agg}} \right) + 1.813 \quad (18)$$

$$f_{t-28 \text{ days}} = \left\{ \frac{2.660 \text{ LM} + 0.202 \text{ SM} - 0.478 \text{ AM}}{\frac{w}{b}} \right\} \left( \frac{b}{\text{agg}} \right) + 3.232 \quad (19)$$

$$f_{t-90 \text{ days}} = \left\{ \frac{3.536 \text{ LM} + 1.058 \text{ SM} - 1.257 \text{ AM}}{\frac{w}{b}} \right\} \left( \frac{b}{\text{agg}} \right) + 2.933 \quad (20)$$

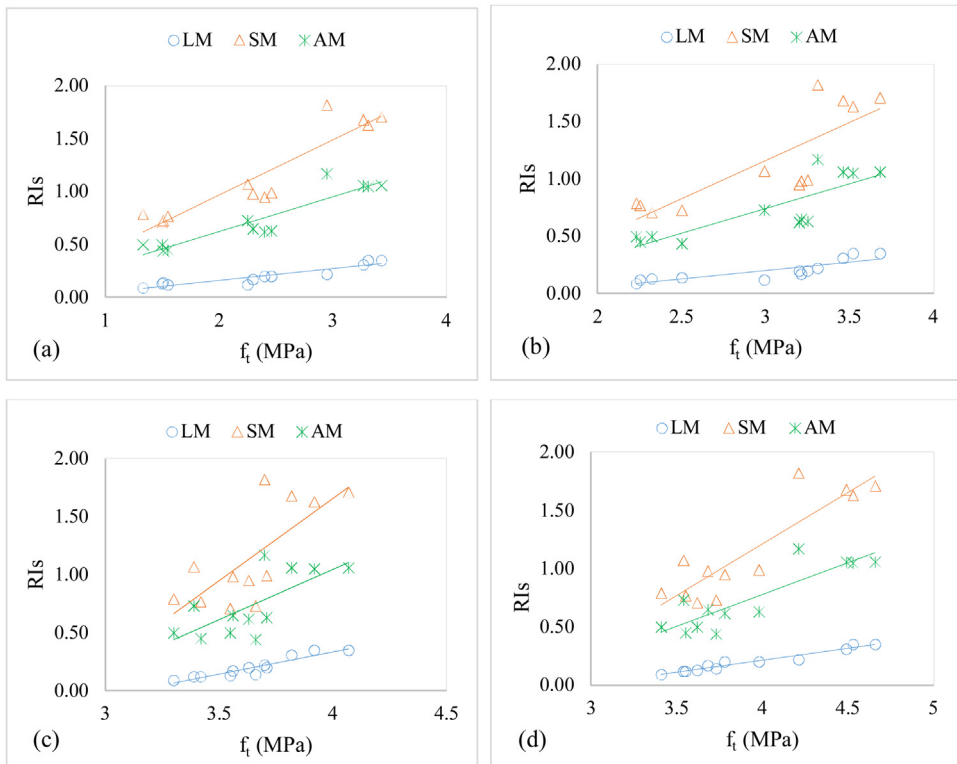


Fig. 10. Statistical data trends between reactivity indexes and splitting tensile strengths at (a) 7, (b) 14, (c) 28, and (d) 90 days.

3.6. Comparison of experimental results with predictive values

Fig. 11 (a)-(c) indicate the statistical compliance tests between the experimental splitting tensile strengths ( $E_{f_t}$ ) and the predictive splitting tensile strength results based on reactivity indexes (RM, HM, and LM) at 28 days curing for M 25, M 30, and M 40, respectively. The predictive splitting tensile strengths were obtained at 28 days curing following the relationships illustrated in Eqs. 11,15,19 for the reactivity modulus (RM), hydraulic modulus (HM), and lime modulus (LM), respectively. The results, as shown in Fig. 11 (a)-(c), yielded strong correlations at 82, 95, and 83 %  $R^2$  for M 25, M 30, and M 40, respectively. An inference can be made that the prediction of concrete splitting tensile strengths incorporating anacardium occidentale (cashew) nutshell ash based on the reactivity indexes and mix design proportions is attainable with a good relationship. Therefore, the model equations developed by this study would be advantageous in the prediction of splitting tensile strength of concrete modified with AONSA by saving time and cost from conducting experimental laboratory works.

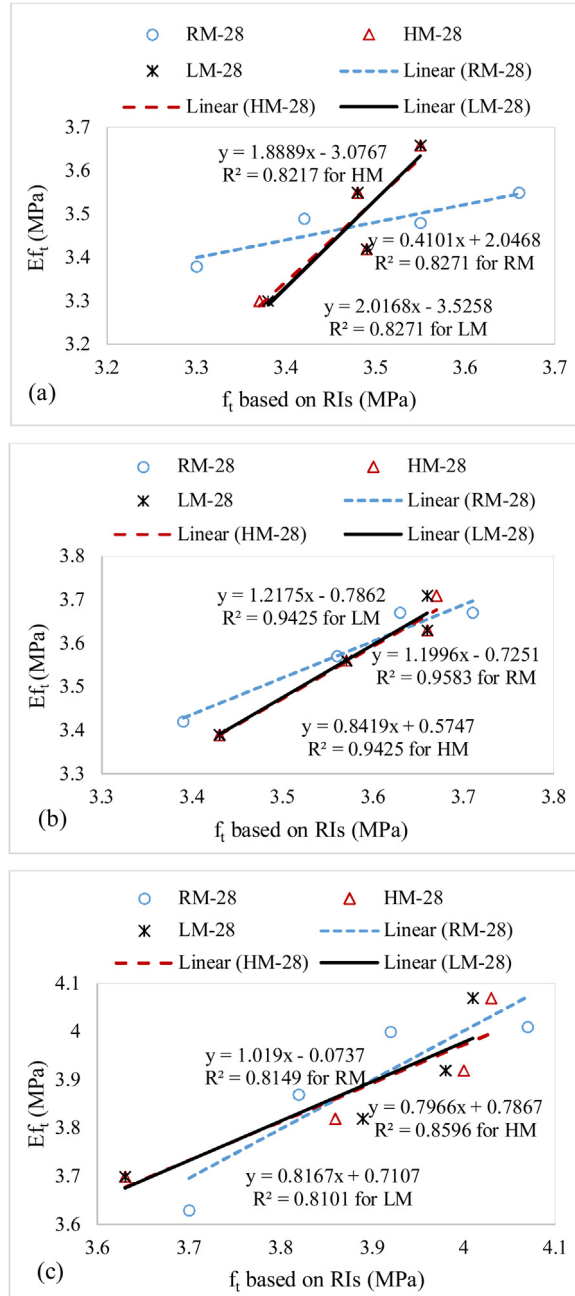


Fig. 11. Statistical comparison of experimental and predictive splitting tensile strengths for (a) grade 25, (b) grade 30, and (c) grade 40 at 28 days curing.

#### 4. Conclusions

The study analyzed the oxide compositions of PLC-AONSA blend using the XRF. The RIs were evaluated, and PLC-AONSA concrete samples were produced. Both experimental works and statistical analysis were engaged, and consequent upon the findings and research aims, the following sets of conclusions are made:

- There was about 3–13 %, 9–29 %, and 10–31 % increase in alumina oxide ( $\text{Al}_2\text{O}_3$ ), and about 16–46 %, 19–46 %, and 15–50 % increase in silica oxide ( $\text{SiO}_2$ ) as the percentage replacement of PLC by AONSA increased from 5 to 20 % for M 25, M 30, and M 40, respectively.
- At 5–20 % AONSA replacement level, lime (CaO) decreased from 31 to 57%, 29–59 %, and 29–58 % for M 25, M 30, and M 40, respectively.
- The reactivity, hydraulic, and lime moduli of PLC-AONSA mixed binder increases with increasing CaO, MgO, and  $\text{Al}_2\text{O}_3$  contents. Both silica and alumina moduli increase with increasing  $\text{SiO}_2$  and  $\text{Al}_2\text{O}_3$  materials, respectively.
- The splitting tensile strength of PLC-AONSA based concrete increases with increasing reactivity indexes.
- The maximum splitting tensile strength occurs at 15 % AONSA substitution.
- The correlation of experimental results with the proposed model equations yields high precision with 82–95 %  $R^2$  at 28 days curing.

The use of reactivity index concepts in the prediction of the splitting tensile strength of PLC-AONSA mix is attainable. The study also affirms the high precision of the fit regression model in the correlation of the splitting tensile strength relative to the reactivity indexes and the mix design proportions of the mix. Therefore, this study offers benefits to future research by focusing on three prospective solutions. First, the developed model equations can be useful in the prediction of the tensile strength of concrete incorporating SCMs against splitting, provided the chemical compositions are obtained. Second, it proffers 15 % of AONSA optimum substitution in green concrete production for structural application. Third, apart from the basic form, AONSA can be used as pozzolanic material for further request.

#### Data availability statement

The authors confirm that the data supporting the findings of this study are available within the article.

#### Declaration of Competing Interest

The authors show a credit to the sources in the manuscript. The authors declare that they have no known competing for financial interests or personal relationships that could have appeared to influence the work reported in this paper. The raw/processed data required to reproduce these findings cannot be shared at this time as the Data also forms part of an ongoing study. The authors declare that the manuscript is the authors' original work and has not been published before. The authors also declare that the article contains no libellous or unlawful statements and does not infringe on the rights of others.

#### Acknowledgements

The authors acknowledge the Covenant University Centre for Research, Innovation, and Discovery (CUCRID) for the provision of the fund and conducive environment in carrying out the study.

#### References

- [1] V.M. Malhotra, Introduction: sustainable development and concrete technology, *ACI Concr. J.* 25 (2002) 1147–1165.
- [2] C. Fan, S.A. Miller, Reducing greenhouse gas emissions for prescribed concrete compressive strength, *Constr. Build. Mater.* 167 (2018) 918–928.
- [3] World Health Organization, World Health Statistics, WHO, Geneva, 2016.
- [4] Sustainable Development Goals, The Sustainable Development Goals Report of the United Nations Statistics Division, (2017) . <https://unstats.un.org/sdgs>.
- [5] E.M. Fairbairn, B.B. Americano, G.C. Cordeiro, T.P. Paula, R.D. Toledo Filho, M.M. Silvano, Cement replacement by sugar cane bagasse ash: CO<sub>2</sub> emissions reduction and potential for carbon credits, *J. Environ. Manag.* 91 (9) (2010) 1864–1871.
- [6] E. Crossin, The greenhouse gas implications of using ground granulated blast furnace slag as a cement substitute, *J. Clean. Prod.* 95 (2015) 101–108.
- [7] E. Aprianti, P. Shafiqh, S. Bahri, J.N. Farahani, Supplementary cementitious materials origin from agricultural wastes: a review, *Constr. Build. Mater.* 74 (2015) 176–187.
- [8] G.C. Isaia, High-performance concrete for sustainable constructions, *Waste Mater. Constr.* 15 (2000) 344–354.
- [9] Food and Agriculture Organization of the United Nations, Food and Agriculture Organization Statistical Pocketbook World Food and Agriculture, (2017) . <http://www.fao.org/3/a-i4691e.pdf>.
- [10] Cashew Handbook, Global Perspective, (2014) . [www.cashewinfo.com](http://www.cashewinfo.com).
- [11] J. Abrego, D. Plaza, F. Luno, M. Atienza-Martinez, G. Gea, Pyrolysis of cashew nutshells: characterization of products and energy balance, *Ener.* 158 (2018) 72–80.
- [12] E.B. Mubofu, From cashew nutshell wastes to high-value chemicals, *Pure Appl. Chem.* 88 (1-2) (2016) 17–27.
- [13] T. Godjo, J.P. Tagutchou, P. Naquin, R. Gourdon, Valorization des coques d'anacarde par pyrolyse au Benin, *Revue Dechets Sciences et Techniques* 70 (2015) 11–18.
- [14] A. Anagonou, V. Songmene, T. Godjo, J. Kouam, Recycling of West African cashew nutshells waste in asphalt concrete: impact on the physicochemical properties of asphalt concrete, *Int. J. Adv. Res. Pub.* 4 (2) (2020) 96–106.



- [15] T. Godjo, L. Vissoh, C. Guidi, A. Adomou, S. Emile, Design of expelling machine for briquettes made of obtained bio-chars from cashew nutshells' pyrolysis, *Int. J. Adv. Res. (Indore)* 4 (12) (2016) 479–485.
- [16] Y. Shi, P.C. Kamer, D.J. Cole-Hamilton, Synthesis of pharmaceutical drugs from cardanol derived from cashew nutshell liquid, *Green Chem.* 21 (2019) 1043–1053.
- [17] G. Venkatakotewararao, S. Baskar, S. Arumugam, Tribological investigation of cashew nut shell oil as a lubricant additive, *IOP Confr, Ser.: Mater. Sci. Eng.* 390 (1) (2018) 012074, doi:<http://dx.doi.org/10.1088/1757-899X/390/1/012074>.
- [18] S. Radhakrishnan, D.B. Munuswamy, S. Devarajan, Effect of nanoparticle on emission and performance characteristics of a diesel engine fueled with cashew nut shell biodiesel, *Ener. Sou. Part A: Recov. Util. Env. Effe.* 40 (20) (2018) 2485–2493.
- [19] G.V. Kasiraman, E. Geo, B. Nagalingam, Assessment of cashew nut shell oil as an alternate oil for compression ignition engines, *Ener.* 101 (2016) 401–410.
- [20] M. Sawadogo, S.T. Tanoh, S. Sidib, N. Kpai, I. Tankoano, Cleaner production in Burkina Faso: a case study of fuel briquettes made from cashew industry waste, *J. Clean. Prod.* 195 (2018) 1047–1056.
- [21] S. Oyeibisi, T. Igba, D. Oniyide, Performance evaluation of cashew nutshell ash as a binder in concrete production, *Case Stud. Constr. Mater.* 11 (2019) e00293.
- [22] K. Pandi, K. Ganesan, Effect of water absorption and sorptivity of concrete with partial replacement of cement by cashew nut shell ash, *Austr. J. Basic Appl. Sci.* 9 (23) (2015) 311–316.
- [23] K. Pandi, R. Anandakumar, K. Ganesan, Study on optimum utilization of groundnut shell ash and cashew nut shell ash in concrete, *Caribb. J. Sci.* 53 (1) (2020) 981–991.
- [24] V. Thirumurugan, S.V. George, K. Dheenadhayalan, Experimental study on the strength of concrete by partial replacement of cement by cashew nut shell ash and chicken feather fibre as fibre reinforcement, *Int. J. Adv. Sci. Res. Dev.* 3 (3) (2018) 238–242.
- [25] N. Farzadnia, A.A. Ali, R. Demirboga, Incorporation of mineral admixtures in sustainable high-performance concrete, *Int. J. Sust. Constr. Eng. Technol.* 2 (1) (2011) 44–56.
- [26] A.K. Parande, B.R. Babu, M.A. Karthik, Study on strength and corrosion performance for steel embedded, *Constr. Build. Mater.* 22 (2008) 127–134.
- [27] M.J. Shannag, High strength concrete containing natural pozzolan and silica fume, *Cem. Concr. Compos.* 22 (2000) 399–406.
- [28] D.G. Nair, A. Fraaij, A.K. Klaassen, A.M. Kentgens, A structural investigation relating to the pozzolanic activity of rice husk ashes, *Cem. Concr. Res.* 38 (2008) 861–869.
- [29] R. Demirboga, Thermal conductivity and compressive strength of concrete incorporation with mineral admixtures, *Build. Environ.* 42 (2007) 2467–2471.
- [30] A. Darquennes, B. Espion, S. Staquet, Assessing the hydration of slag cement concretes, *Constr. Build. Mater.* 40 (2013) 1012–1020.
- [31] E. Sakai, S. Miyahara, S. Ohsawa, S.H. Lee, M. Daimon, Hydration of fly ash cement, *Cem. Concr. Res.* 35 (6) (2005) 1135–1140.
- [32] M. Behim, M. Beddar, P. Clastes, Reactivity of granulated blast furnace slag, *Slovak J. Civ. Eng.* 21 (2) (2013) 7–14.
- [33] A.M. Neville, *Properties of Concrete*, fifth ed., Pearson Education Ltd., England, 2011.
- [34] G.I. Obiefuna, P.H. Sini, A. Maunde, Geochemical and mineralogical composition of granitic rock deposits of Michika area North East, Nigeria, *Int. J. Sci. Technol. Res.* 7 (4) (2018) 160–170.
- [35] A. Rittman, Using the Rittman serial index to define the alkalinity of igneous rocks, *E Schwetzerbartsche Vealagsbuchandlung Stuttgart* 184 (1) (1962) 95–103.
- [36] T. Xie, P. Visintin, A unified approach for mix design of concrete containing supplementary cementitious materials based on reactivity moduli, *J. Clean. Prod.* 203 (2018) 68–82.
- [37] S.U. Khan, M.F. Nuruddin, T. Ayub, N. Shafiq, Effects of different mineral admixtures on the properties of fresh concrete, *Transfus. Apher. Sci.* 986567 (2014) 1–11, doi:<http://dx.doi.org/10.1155/2014/986567>.
- [38] A.S.T.M.C. 25-06, Standard Test Methods for Chemical Analysis of Limestone, Quicklime, and Hydrated Lime, ASTM International, West Conshohocken, PA, 2006, pp. 36.
- [39] British Standard E.N. 196-3, Method of Testing Cement: Physical Test, London, BSI, 2016.
- [40] British Standard E.N. 196-6, Methods of Testing Cement: Determination of Fineness, BSI, London, 2018.
- [41] J. Bijen, Benefits of slag and fly ash, *Constr. Build. Mater.* 10 (5) (1996) 309–314.
- [42] M. Thomas, R.D. Hooton, C. Rogers, B. Fournier, 50 years old and still going strong, *Concr. Int.* 34 (2012) 35.
- [43] British Standard E.N. 12620, Aggregates from Natural Sources for Concrete, BSI, London, 2013.
- [44] S. Donatello, M. Tyrer, C.R. Cheeseman, Comparison of test methods to assess pozzolanic activity, *Cem. Concr. Compos.* 32 (2010) 121–127.
- [45] British Standard E.N. 450-451, Pozzolan for use in Concrete: Definitions, Specifications and Conformity Criteria, BSI, London, 2012.
- [46] British Standard E.N. 8615-2, Specification for Pozzolanic Materials for use with Portland Cement: High Reactivity Natural Calcined Pozzolana, BSI, London, 2019.
- [47] American Society for Testing and Materials C 618, Standard Specification for Coal Fly Ash and Raw or Calcined Natural Pozzolan for use in Concrete, ASTM, 2012.
- [48] S.A. Lima, J.A. Rossignolo, H.S. Junior, Analysis of the cashew nut production waste for use in cement composites, *Pro-Africa Conf.: Non-Conv. Build. Mater. Agro. Ind. Wastes, Pirassununga - SP, Brazil* 18–19 (2010) 112–119.
- [49] British Standard EN 3892-1, Pulverised-fuel Ash: Specification for Pulverised Fuel Ash for Use With Portland Cement, BSI, London, 1997.
- [50] British Standard EN 206, Concrete Specifications, Performance, Production and Conformity, BSI, London, 2016.
- [51] British Standard 1881-125, Testing Concrete: Methods for Mixing and Sampling Fresh Concrete in the Laboratory, BSI, London, 2013.
- [52] British Standard E.N. 12390-12392, Testing Hardened Concrete: Making and Curing for Strength Tests, BSI, London, 2019.
- [53] British Standard E.N. 12350-12352, Testing Fresh Concrete: Method for Determination of Slump, BSI, London, 2009.
- [54] British Standard E.N. 12390-12393, Testing Hardened Concrete: Compressive Strength of Test Specimens, BSI, London, 2009.
- [55] British Standard E.N. 12390-12396, Testing Hardened Concrete: Splitting Tensile Strength of Test Specimens, BSI, London, 2019.
- [56] Q. Yu, K. Sawayama, S. Sugita, M. Shoya, Y. Isojima, Reaction between rice husk ash and Ca(OH)<sub>2</sub> solution and the nature of its product, *Cem. Concr. Res.* 29 (1) (1999) 37–43.
- [57] K. Pandi, R. Anandakumar, K. Ganesan, Study on optimum utilization of groundnut shell ash and cashew nut shell ash in concrete, *Caribb. J. Sci.* 53 (1) (2020) 981–991.
- [58] P.L. Owens, Fly ash and its usage in concrete, *Concr.* 13 (7) (1979) 21–26.
- [59] J. Dewar, The Particle Structure of Fresh Concrete-A New Solution to an Old Question, First Sir Frederick Lea Memorial Lecture 986 (1986) 23.
- [60] S. Wild, J.M. Khatib, A. Jones, Relative strength, pozzolanic activity and cement hydration in superplasticized metakaolin concrete, *Cem. Concr. Res.* 26 (10) (1996) 1537–1544.
- [61] British Standard E.N. 1992-1-1, Design of Concrete Structures: General Rules for Structural Fire Design, BSI, London, 2014.
- [62] I.I. Akinwumi, O.I. Aidomogie, Effect of corncob ash on the geotechnical properties of lateritic soil stabilized with Portland cement, *Int. J. Geomat. Geosci.* 5 (3) (2015) 375–392.